

## 秋田大学研究グループの成果が米国の「Journal of Functional Foods」にオンライン掲載 カレーのスパイス「クルクミン」が熱変性した GO-Y022 が胃癌を抑制することを解明

秋田大学大学院医学系研究科臨床腫瘍学講座・腫瘍内科の柴田浩行教授と吉田泰一医員の研究グループは東北大学、金沢大学、癌研究会癌研究所との共同研究により、スパイスのクルクミンが熱変性によってできる化合物”GO-Y022”がヒトの胃癌細胞株の増殖を抑制し、アポトーシスによる細胞死を誘導することを発見しました。また、胃癌を起こすモデルマウスに GO-Y022 を含む餌を経口摂取させると、GO-Y022 を含まない餌を投与した胃癌モデルマウスと比較して胃癌のサイズが約 1/3 に縮小されました。GO-Y022 は市販のカレーにも含まれていました。今後、「GO-Y022 リッチなカレー」のメニューを考案することなどで医食同源を目指すことが期待されます。

本研究成果は 10 月 17 日に Journal of Functional Foods のオンラインで (<https://authors.elsevier.com/a/1Xv9U6FNx9edP9>) 公表されました。

胃癌による死亡は世界第 2 位を占める悪性腫瘍です。クルクミンは癌化に関連する分子を抑制することが知られています。しかし、クルクミンの活性は低く、改良の余地があります。そこで、我々は様々なクルクミンの誘導体を合成し、抗腫瘍活性が強い誘導体の合成に成功しました。しかし、これらの誘導体はペンタノイドであり、ヘプタノイドであるクルクミンとは化学構造が大きく異なっていました。近年、これらの誘導体の中で GO-Y022 と名付けたペンタノイドがクルクミンの熱変性で生じることが判明しました。この GO-Y022 は 4 種類の胃癌細胞株に対してクルクミンよりも約 5 倍強い抗腫瘍活性を示し、また、GO-Y022 はクルクミンよりも強いアポトーシス誘導能を有しています。GO-Y022 は胃癌のマウスモデルの腫瘍のサイズを約 1/3 に抑制し、経口摂取された GO-Y022 は胃の粘膜や胃癌で検出されましたが、血液中には見出されませんでした。GO-Y022 は胃粘膜で作用し、全身性の有害事象も認められませんでした。GO-Y022 は市販のカレーにも含まれ、GO-Y022 には胃癌の抑制効果があり、実はこれまでもカレーの成分として食べられていました。これによりカレーの GO-Y022 は機能性食品になりうる可能性が示されました。

【論文著者・タイトル】

Taichi Yoshida, Takashi Maruyama, Masatomo Miura, Masahiro Inoue, Koji Fukuda,  
Kazuhiro Shimazu, Daiki Taguchi, Hiroaki Kanda, Masanobu Oshima, Yoshiharu Iwabuchi,  
Hiroyuki Shibata

Dietary intake of pyrolyzed deketene curcumin inhibits gastric carcinogenesis

【お問い合わせ先】

秋田大学大学院医学系研究科

臨床腫瘍学講座 教授 柴田浩行

TEL : 018-884-6261

FAX : 018-884-6455

E-mail : m-soumu@hos.akita-u.ac.jp



## Dietary intake of pyrolyzed deketene curcumin inhibits gastric carcinogenesis

Taichi Yoshida<sup>a</sup>, Takashi Maruyama<sup>b</sup>, Masatomo Miura<sup>c</sup>, Masahiro Inoue<sup>a</sup>, Koji Fukuda<sup>a</sup>, Kazuhiro Shimazu<sup>a</sup>, Daiki Taguchi<sup>a</sup>, Hiroaki Kanda<sup>d</sup>, Masanobu Oshima<sup>e</sup>, Yoshiharu Iwabuchi<sup>f</sup>, Hiroyuki Shibata<sup>a,\*</sup>

<sup>a</sup> Department of Clinical Oncology, Graduate School of Medicine, Akita University, Akita, Japan

<sup>b</sup> Department of Immunology, Graduate School of Medicine, Akita University, Akita, Japan

<sup>c</sup> Department of Pharmacy, Akita University Hospital, Akita, Japan

<sup>d</sup> Division of Pathology, Cancer Institute, Japanese Foundation for Cancer Research, Tokyo, Japan

<sup>e</sup> Division of Genetics, Cancer Research Institute, Kanazawa University, Kanazawa, Japan

<sup>f</sup> Department of Organic Chemistry, Graduate School of Pharmaceutical Science, Tohoku University, Sendai, Japan

### ARTICLE INFO

#### Keywords:

Curcumin  
Chemoprevention  
Diarylpentanoid analog  
Gastric cancer  
Pyrolysis  
STAT3 inhibition

### ABSTRACT

Gastric cancer is the second leading cause of cancer-related mortality worldwide. Curcumin, a phytochemical, possesses molecular inhibitory potentials for regulating malignancies. However, the lower potential of curcumin warrants improvement. Thus, we synthesized diarylpentanoid analogs with higher potency; however, these differed structurally from curcumin—a heptanoid. Recently, one diarylpentanoid was formed following pyrolysis of curcumin, which is identical to our GO-Y022. The growth inhibition of gastric cancer cells by GO-Y022 was five-fold higher than by curcumin; GO-Y022 displayed superior apoptosis induction ability. Besides, it suppressed the gastric tumor growth to a third in a mouse model. GO-Y022 was moved to the epithelial and gastric tumors but not detected in the bloodstream. Moreover, oral GO-Y022 was effective topically, exhibited no adverse events in mice, and was detected in the commercially available curry paste. Briefly, GO-Y022 can inhibit gastric carcinogenesis; it is dietary and can be safely used as an oral functional food.

### 1. Introduction

Gastric cancer is the second leading cause of cancer-related mortality globally, with a mortality rate of 700,000 in 2012 (Ferlay, Soerjomataram, & Dikshit, 2015). Typical risk factors for gastric cancer comprise *Helicobacter pylori* infection, obesity, smoking, consumption of red meat and alcohol, and low socioeconomic status (Hundahl, Phillips, & Menck, 2000). However, the precise mechanisms underlying gastric cancer remain unclear, necessitating the determination of effective treatment for gastric cancer. Surgical resection, the only approach for a cure, is not applicable in patients with stage IV gastric cancer, for whom chemotherapy remains the primary treatment (Japanese Gastric Cancer Association, 2017). However, the median survival of stage IV patients is approximately 1 year at best, even with the use of the newer treatment options (Cunningham, Starling, & Rao, 2008; Van Cutsem, Moiseyenko, & Tjulandin, 2006).

Previously, several dietary elements, such as phytochemicals, have

been investigated for cancers in these aspects. Curcumin, a dietary pigment in use for > 3000 years in Asia primarily, is being increasingly analyzed for its antitumor potential (Kunnumakkara, Bordoloi, & Harsha, 2017). Reportedly, curcumin can suppress the proliferation of various cancer cell types and induce apoptosis (Kunnumakkara et al., 2017). In addition, it comprises antiangiogenic properties and is known to enhance cancer immunity and inhibit cancer immunotolerance (Mohamed, Jantan, & Haque, 2017). Furthermore, curcumin inhibits the growth of gastric cancer cell lines (Zhang, Lin, & Zhou, 2015). However, curcumin is not used in a clinical setting because of its limited bioavailability and relatively low potential, and the ongoing research is focused on overcoming these limitations.

Thus, we successfully synthesized a series of new diarylpentanoid analogs to attain a new curcumin analog with higher antitumor potential (Ohori, Yamakoshi, & Tomizawa, 2006) and demonstrated that the new analogs inhibited the proliferation of various cancer cell types, including colon cancer stem cells (Lin, Liu, & Li, 2011). In addition, we

**Abbreviations:** C5, diarylpentanoid; STAT3, signal transducers and activators of transcription 3

\* Corresponding author at: Department of Clinical Oncology, Graduate School of Medicine, Akita University, Hondo 1-1-1, Akita, Japan.

E-mail address: [hiroyuki@med.akita-u.ac.jp](mailto:hiroyuki@med.akita-u.ac.jp) (H. Shibata).

<https://doi.org/10.1016/j.jff.2018.09.033>

Received 2 June 2018; Received in revised form 29 September 2018; Accepted 30 September 2018

1756-4646/ © 2018 Elsevier Ltd. All rights reserved.

determined that these analogs exhibited the safety profile of the original compound curcumin in mouse models (Lin et al., 2011; Shibata, Yamakoshi, & Sato, 2009) and that one diarylpentanoid, 1,5-bis(3,5-dimethoxy-4-methoxymethoxyphenyl)pentadien-3-one (GO-Y031) inhibited gastric carcinogenesis *in vivo* with a good safety profile (Uehara, Inoue, & Fukuda, 2014). However, a big gap remains between the mouse models and the first-in-human study. Our diarylpentanoid analogs (C5) are structurally different from curcumin, which is a diarylheptanoid (C7). Recently, a breakthrough finding was reported demonstrating that a deketene form of curcumin, which is a C5 analog, formed because of curcumin pyrolysis during cooking of curry (Dahmke, Boettcher, & Groh, 2014), this C5 analog is identical to an analog we synthesized, 1,5-bis(4-hydroxy-3-methoxyphenyl)-1,4-pentadiene-3-one (GO-Y022). Thus, this study aims to investigate the efficacy and safety of GO-Y022 in human gastric cancer cell lines and a mouse gastric cancer model and determines the pharmacokinetic profile of GO-Y022.

## 2. Material and methods

### 2.1. Compounds

Originally, GO-Y022 was synthesized by the Department of Organic Chemistry, Graduate School of Pharmaceutical Science at Tohoku University (Sendai, Japan) and was subsequently purchased from Nippon Carbide Industries Co., Inc. (Tokyo, Japan; Fig. 1). We dissolved GO-Y022 in dimethyl sulfoxide (DMSO) at 10–50 mmol/L as a stock solution. Curcumin was purchased from Wako Pure Chemical Industries (Osaka, Japan), and the high-fat diet (HFD) 32 was purchased from CLEA Japan (Tokyo, Japan).

### 2.2. Cell lines

We obtained the gastric cancer cell lines KATO III and GCIY from the American Type Culture Collection through Summit Pharmaceutical International (Tokyo, Japan) and RIKEN BioResource Research Center (Tsukuba, Japan), respectively. In addition, both H-111-TC and SH-10-TC were obtained from Cell Resource Center for Biomedical Research Cell Bank Tohoku University. Notably, all cell lines were cultured per the manufacturer's protocols.

### 2.3. *In vitro* growth assay

We assayed the cell viability by quantification of the uptake and metabolism of WST-8 (2-(2-methoxy-4-nitrophenyl)-3-(4-nitrophenyl)-5-(2,4-disulfophenyl)-2H-tetrazolium monosodium salt), per the manufacturer's instructions (Dojindo Laboratories, Kumamoto, Japan). Then, we determined the half-maximal inhibitory concentration (IC<sub>50</sub>) by the MTT assay as described previously (Kudo, Yamakoshi, & Sato, 2011).

### 2.4. Effect on a normal gastric epithelial cells

A human gastric epithelial cells from 58 year Caucasian, HGaEpC was purchased from CELL APPLICATIONS, INC (San Diego, CA). HGaEpC cells (lot 3288) were seeded in each well of a 96 well-plate at  $5 \times 10^5$  cells. Cells were cultured with the manufactures' supplied

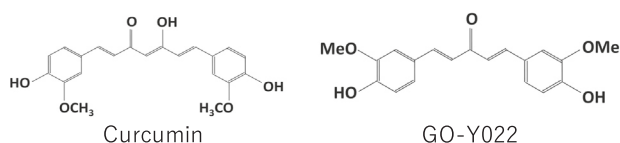


Fig. 1. Schematic diagrams of curcumin and GO-Y022. MeO indicates a methoxy group.

medium added by GO-Y022, and the IC<sub>50</sub> values were calculated after 72 h incubation.

### 2.5. Apoptosis analysis

Cells were cultured in a 10 cm-dish to semiconfluency, then they were treated with GO-Y022 at the indicated concentration. After 24 h treatment, cells were lysed and the lysate was applied to the ELISA plate. Apoptosis was determined by the M30-Apoptosense enzyme-linked immunosorbent assay (ELISA; VLVbio) from Funakoshi (Tokyo, Japan), per the manufacturer's protocol. We treated the control with 1% DMSO alone. The relative values were calculated as the ratio to the control (the control value = 1.0). All cellular experiments were conducted in triplicate, unless otherwise specified.

### 2.6. ELISA ( $\beta$ -catenin and STAT3)

Cells were cultured in a 10 cm-dish to semiconfluency, then they were treated with GO-Y022 at the indicated concentration. After 24 h treatment, cells were lysed and the lysate was applied to the ELISA plate. We determined the activation of  $\beta$ -catenin and phosphorylation of signal transducers and activators of transcription 3 (STAT3) using the Active  $\beta$ -Catenin MKA ELISA (Symansis, New Zealand) and phospho-STAT3 (pSTAT3) Tyr705 sandwich ELISA (Cell Signaling Technology Japan, Tokyo, Japan), respectively. The obtained values were corrected by the cell numbers and then represented as the relative values against the control (the control value = 1.0).

### 2.7. Fluorescence-activated cell sorting (FACS) analysis

Cells were seeded in a 6 well plate to grow semi-confluent. Then, they were treated with compounds for 48 h. Cells were scraped and stained with Annexin V apoptosis detection kit APC (Invitrogen, Thermo Fisher Scientific K.K. Tokyo, Japan) and propidium iodide (eBioscience, Thermo Fisher Scientific K.K.) to detect apoptosis/necrosis, according to the manufacturer's protocol. The stained cells were subjected to flow cytometric analysis with BD FACS Aria™ III (BD bioscience, Tokyo, Japan). Data were analyzed with FlowJo software (Tree Star, OR).

### 2.8. Mice experiments

We obtained K19-Wnt1/C2 mE (Gan) mice by crossing K19-Wnt1 and K19-C2 mE mice (Oshima, Matsunaga, & Fujimura, 2006). Gan mice are genetically engineered animals where activated oncogene, Wnt-1 signaling and inflammation related genes such as COX-2 and prostaglandin E synthase, are up-regulated simultaneously. Resulting gastric cancers arise spontaneously. Every day, Gan mice were fed 5 g High Fat Diet 32 alone ( $n = 6$ ) or HFD added with 0.5% (weight/weight) GO-Y022 ( $n = 7$ ), starting since 9 weeks of age and were sacrificed and examined at 16 weeks of age with minor modifications, as described previously (Uehara et al., 2014). As shown in the previous study, gastric cancer could be detected after 12-weeks of age in the HFD-fed Gan mice (Uehara et al., 2014). HFD was used, because GO-Y022 is hydrophobic, and it can be mixed well with oily materials, such as HFD. All animal experiments were performed humanely and complied with the guidelines set by Akita University and were approved by the related ethics committee (certification #a-1-2641). The tumor volumes were evaluated as follows (Euhus, Hudd, & LaRegina, 1986): tumor volume (mm<sup>3</sup>) = (shortest tumor diameter)<sup>2</sup> × (longest tumor diameter)/2.

### 2.9. Immunohistochemistry

We performed immunohistochemistry as previously described (Uehara et al., 2014) using previously described protocols with the following antibodies: anti-mouse  $\beta$ -catenin (1:1500; C2206, rabbit;

Sigma-Aldrich, Tokyo, Japan) and anti-mouse pSTAT3-Tyr705 (1:100; D3A7, rabbit; Cell Signaling Technology, Japan) (Uehara et al., 2014). To Quantitate the positivity of pStat3 expression, we randomly selected the specimen and over 80 epithelial cells were counted for the positivity of pStat3 in each mouse group (HFD diet mice; n = 7, GO-022 diet mice; n = 6), and the percentage of positivity is indicated.

## 2.10. Evaluation of the safety profile of GO-Y022

As a measure of the overall health status, body weight of mice was determined before sacrifice. In addition, the tissue-specific toxicity profile of GO-Y022 was assessed by a blood test. Briefly, we collected blood from the infraorbital venous plexus before sacrifice and analyzed the serum by Oriental Yeast (Tokyo, Japan) to evaluate the total bilirubin (T-Bil), aspartate aminotransferase (AST), and alanine aminotransferase (ALT) for liver toxicity, creatinine (Cre) for renal toxicity, and lactate dehydrogenase (LDH).

## 2.11. Localization of GO-Y022

We determined tissues localization and blood concentrations of GO-Y022. Briefly, at the time of sacrifice, we collected specimens from the heart, kidney, liver, spleen, and digestive tract, including the esophagus, stomach, and small and large intestines, as well as the gastric tumor. Resected alimentary tracts were incised along their long axis, and washed in the distilled water with vigorous shaking to remove the feed of the surface several times. Then, the tracts were expanded with pins on the dork board. The mucosal surface was swabbed by cotton wetted with the distilled water until the all oily content of High Fat Diet was disappeared. After measuring the weight of the tissue sample, then they were homogenized in the distilled water, and analyzed by HPLC. The parenchymal organs were directly homogenized in the distilled water.

The sample of each tissue was homogenized in 200  $\mu$ L of the distilled water, and it was applied to an Oasis HLB extraction cartridge (Nihon Waters K.K., Tokyo, Japan) that was preactivated with

methanol and water (1.0 mL each). Next, we washed the cartridge with 1.0 mL water and 1.0 mL 60% methanol in water and eluted with 1.0 mL 100% methanol. Then, the eluate was dried by vortex-vacuum evaporation at 70 °C using a rotary evaporator (AS-ONE CVE-2AS, Osaka, Japan). After that, we dissolved the resulting residue in 20  $\mu$ L methanol and vortexed for 30 s; in addition, 20  $\mu$ L of the mobile phase was added to the sample, which was vortexed for another 30 s. Next, we processed a 20  $\mu$ L aliquot of the sample by high-performance liquid chromatography (HPLC), which was conducted using a PU-2080 plus chromatography pump (JASCO, Tokyo, Japan) equipped with a CAPCELL PAK C18 MG II (250 mm  $\times$  4.6 mm I.D.; Shiseido, Tokyo, Japan) HPLC column, a UV-2075 light source, and an ultraviolet detector (JASCO). The mobile phase was water–acetonitrile–methanol (55:25:20, v/v/v), which was degassed in an ultrasonic bath before using. In addition, the flow rate was 0.5 mL/min at ambient temperature, and we performed the sample detection at 250 nm. The amount of GO-Y022 was corrected by the tissue wet weight, and indicated as ng/g tissue. Of note, we also measured blood concentrations of GO-Y022 as bellow. Five milligram of GO-Y022 (mixed with 200  $\mu$ L of 1% methyl cellulose (Wako)) was orally administrated by using a flexible sonde (5202, FUCHIGAMI, Kyoto, Japan) to the twelve week-aged B6 male mice, which were anesthetized with intraperitoneal injection of 50  $\mu$ L of the mixture of 10 mg of midazolam (SANDOZ, Tokyo, Japan), 0.75 mg of medetomidine (ZENOAQ, Koriyama, Japan), and 12.5 mg of butorphanol (Wako) dissolved in 25 mL of distilled water after one-day fasting. Blood samples were collected at 1, 2, 4, 8 and 24 h after administration (n = 3). The same amount of 200  $\mu$ L of 1% methyl cellulose alone was orally administrated to the control group mice under same anesthesia, and the blood samples were obtained at the same intervals (n = 3). The blood concentration of GO-Y022 and their metabolites were determined by following HPLC method. After addition of 200  $\mu$ L acetonitrile a 50  $\mu$ L blood sample, the solution was vortexed for 30 s. This mixture was spun for 5 min at 13,000g. The clear supernatant was filtered through a Millipore filter (0.45  $\mu$ m; Millex-LH<sup>®</sup>, Tokyo, Japan) and was then injected into the HPLC apparatus.

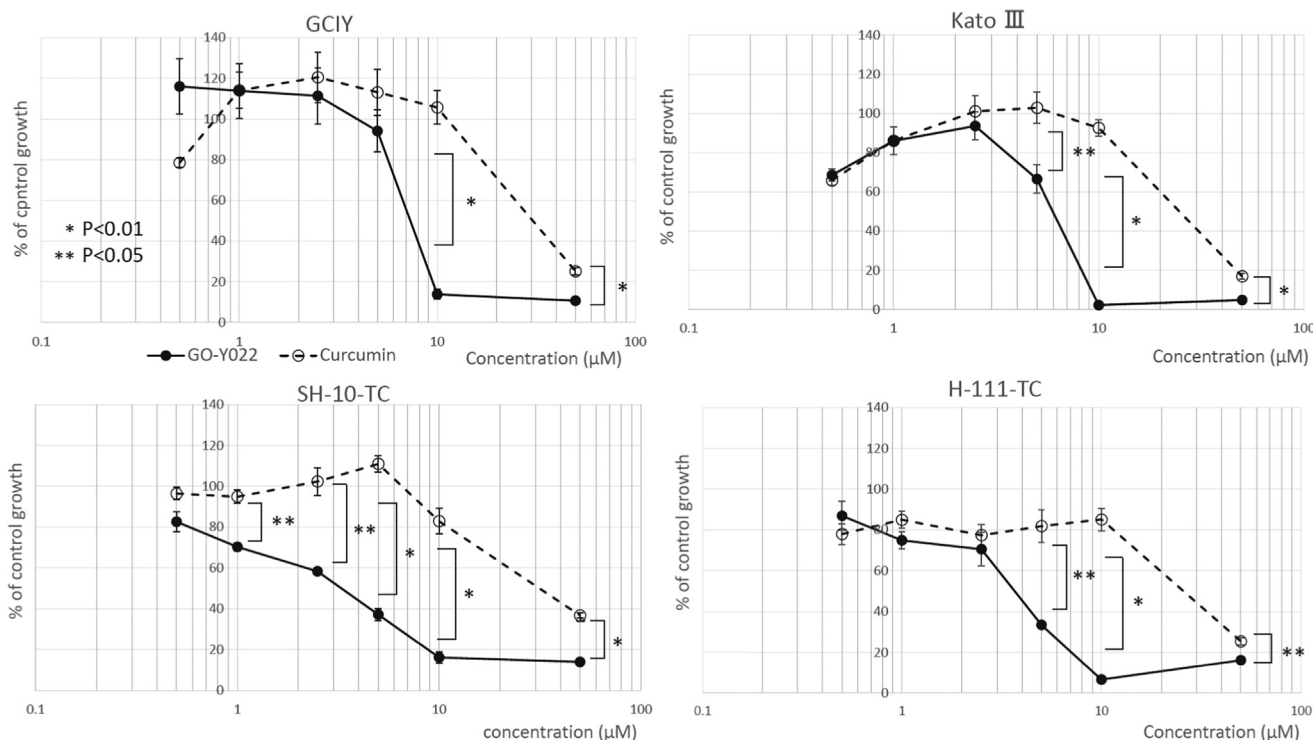


Fig. 2. The growth inhibition of gastric cancer cell lines treated with GO-Y022. The growth inhibition was calculated as the percentage of the cell numbers against the mock (vehicle alone, 1% DMSO). Open circle indicates curcumin, and the closed circle indicates GO-Y022. \*  $P < 0.01$ ; \*\*  $P < 0.05$ .

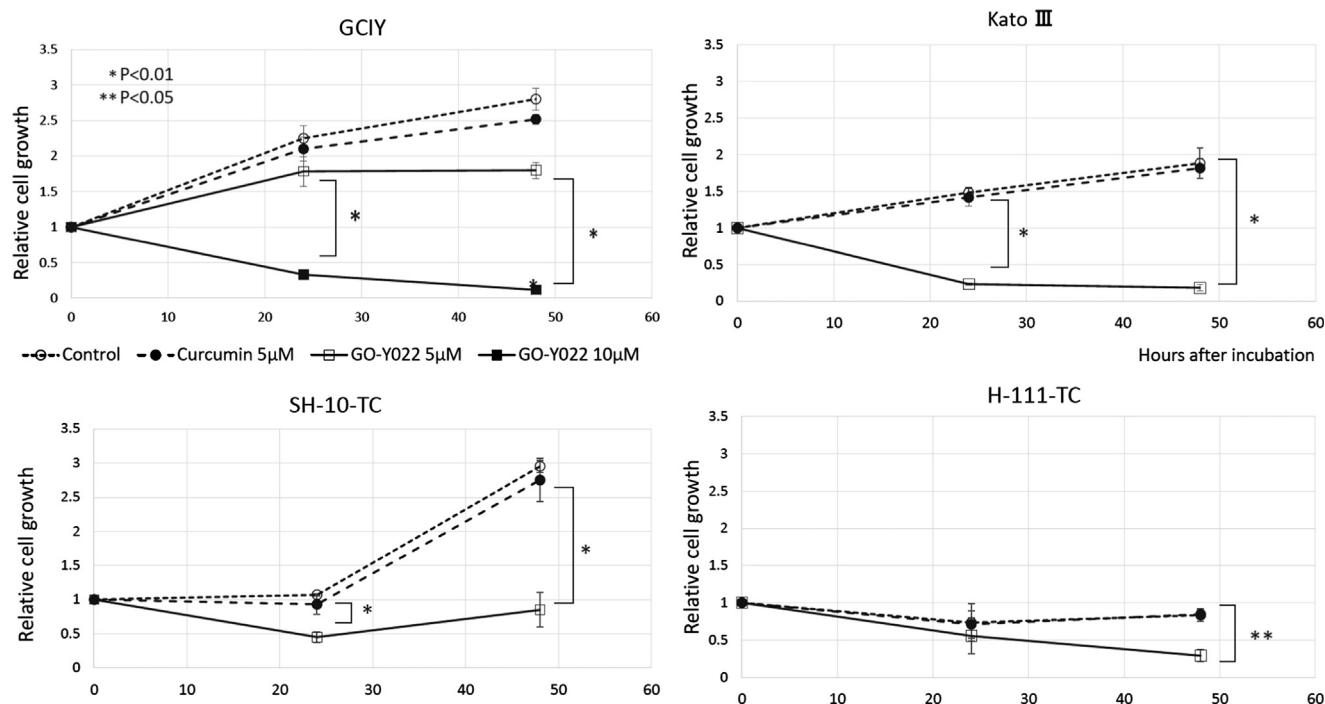


Fig. 3. Growth properties of gastric cancer cell lines treated with GO-Y022. Control cultures were treated with the vehicle alone (1% DMSO). The starting cell number (at 0 hr) is indicated as 1.0, and the cell numbers are indicated as relative values to the start. Open circle indicates the control. Closed circle indicates 5 µM of curcumin treatment. Open rectangle indicates 5 µM of GO-Y022 treatment. Closed rectangle indicates 10 µM of GO-Y022 treatment.  $P < 0.01$ ;  $**P < 0.05$ .

## 2.12. Mass spectrometry

Quantification of GO-Y022 in curry was outsourced to Japan Food Research Laboratories (Tokyo, Japan). The procedures were described briefly. GO-Y022 was dissolved in methanol, and diluted with water/methanol (1:1) solution to make standard solution ranging 0.0001–0.01 mg/L. Five gram of curry sample was mixed with 20 mL of hexane, then homogenized with 40 mL of hexane saturated acetonitrile. After centrifugation (2000g, 5 min), the under (acetonitrile) layer was collected. Then, remaining hexane layer was again mixed with 40 mL of acetonitrile, and centrifuged. This step was repeated two times. The collected acetonitrile layer was mixed. The volume was measured, and one of 200 mL was applied to Sep-Pak Plus C18 column (Waters, Tokyo, Japan) conditioned by acetonitrile. Then, the sample was eluted with 1 mL of acetonitrile. The eluent was dried, then solved in 2 mL of water/methanol (1:1) solution, and finally it was diluted with water/methanol (1:1) to 5-fold dilution. Two microliter of sample solution was analyzed by liquid chromatography-tandem mass spectrometry (LC unit: Agilent 1100 series (Agilent Technologies, Tokyo, Japan), MS unit: API-4000 (Applied Biosystems, Waltham, MA)). The operation condition was described below: column (CAPCELL PAK C18 MG II (SHISEIDO, Tokyo, Japan)), column temperature (40 °C), mobile phase (A; 0.1 vol% formic acid-acetonitrile, B; 0.1 vol% formic acid solution)

Time (min)	0	2	7.5	7.51	15
Phase A (%)	55	95	95	55	55
Phase B (%)	45	5	5	45	45

Flow rate: 0.2 mL/min, Injection volume: 2 µL, Ionization mode: ESI (+), Curtain gas: 40 psi, Nebulizer gas: 60 psi, Drying gas: 70 psi, Drying gas temperature: 650 °C, Collision gas: nitrogen, Ionization: 5000 V, Declustering potential: 86 V, Multiple reaction monitoring transition (m/z), collision energy (eV): 327.2 > 89.2 (65), 327.2 > 145.1 (39), 327.2 > 177.2 (29).

Pyrolysis was conducted by heating 100 g of curry roux by microwave (250 °C for 20 min).

## 2.13. Statistical analysis

Data are presented as mean  $\pm$  standard deviation. The between-group differences were analyzed using the Fisher's exact probability test or unpaired Student's *t*-test (two-sided) with StatMate III version 3.14 (ATMS, Tokyo, Japan) or BellCurve for Excel version 2.00 (Tokyo, Japan).

## 3. Results

### 3.1. GO-Y022 suppressed the growth of gastric cancer cell lines

We examined the growth inhibitory potential of GO-Y022 in four gastric cancer cell lines, including GCIY, KATO III, SH-10-TC, and H-111-TC. The  $IC_{50}$  value for GO-Y022 after 96 h treatment for GCIY was 7.32 µM, whereas that for curcumin were 30.4 µM. That of GO-Y022 for KATO III was 5.98 µM, whereas that of curcumin for KATO III was 24.8 µM. Those of GO-Y022 were 3.28 µM for SH-10-TC, and 3.67 µM for H-111-TC, respectively, whereas those of curcumin were 31.5 µM for SH-10-TC, and 25.8 µM for H-111-TC, respectively. The inhibition of growth was significantly higher with GO-Y022 than curcumin in all four gastric cancer cell lines (Fig. 2). The  $IC_{50}$  value was 4.2-fold higher in GCIY, and 4.1-fold higher in KATO III. Those were 9.6-, and 7.0-fold higher in SH-10-TC, and H-111-TC, respectively. In addition, the average  $IC_{50}$  of GO-Y022 was  $5.06 \pm 1.88$  µM, which was significantly lower than that of curcumin ( $27.4 \pm 3.55$  µM;  $P < 0.001$ ). These *in vitro* findings suggested that the growth inhibitory potential of GO-Y022 was 5.4-fold higher than that of curcumin.

Next, we assessed the growth property of each gastric cancer cell line in the presence of 5 µM GO-Y022. The same concentration of curcumin could not inhibit the growth at 24 h following the treatment for all four cell lines (Fig. 3). Except for GCIY, 5 µM GO-Y022 decreased the growth < 50% of the control for three cell lines at 24 h (Fig. 3). For GCIY, 10 µM GO-Y022 decreased the growth < 50% of the control (Fig. 3). In addition, three of four gastric cancer cell lines could not grow in the presence of 5 µM GO-Y022, whereas those could grow in the

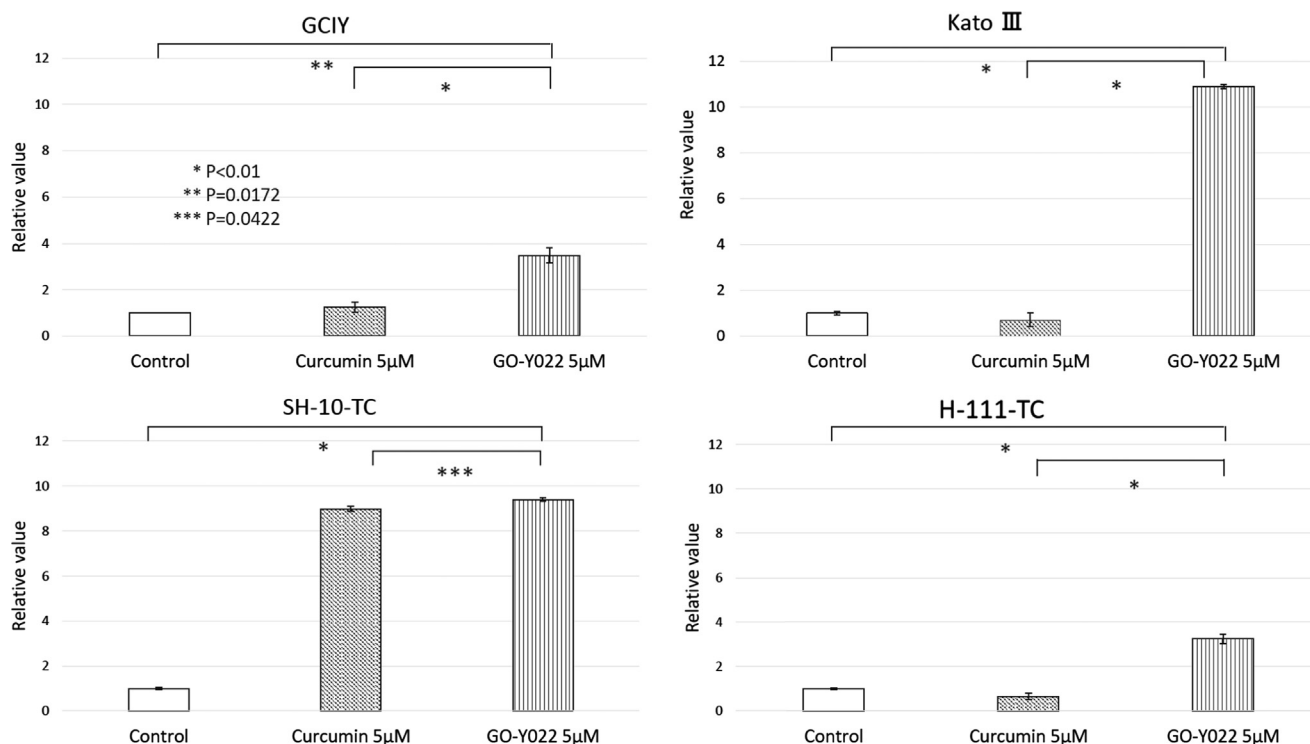


**Fig. 4.** The apoptosis induction with GO-Y022 in gastric cell lines. The amount of an apoptosis indicator, soluble caspase-cleaved keratin 18 was determined by ELISA. The amount of soluble caspase-cleaved keratin 18 in the mock-treated cells (control) is indicated as 1.0. The relative values to the mock were indicated in each treated cells with 5 µM of curcumin or GO-Y022. The statistical significance is indicated by asterisks.

presence of 5 µM curcumin. Overall, these findings suggested that GO-Y022 exhibited a stronger growth inhibitory potential than curcumin.

### 3.2. Apoptosis induction with GO-Y022

We assessed the amount of an apoptosis indicator, soluble caspase-cleaved keratin 18 by ELISA at 24 h after treatment. And those amounts were compared with the mock-treated cells (control) was indicated as 1.0. These relative apoptosis levels to the mock were indicated in each

treated cells.

After 24 h treatment, the mean relative level of apoptosis in GCIY cells treated with 5 µM GO-Y022, evaluated per the rate of apoptosis in cultures treated with the vehicle DMSO that was set to 1.0, was  $3.48 \pm 0.64$ , whereas that with 5 µM curcumin was  $1.25 \pm 0.42$  (Fig. 4). For KATO III, the relative apoptosis level was  $10.85 \pm 0.21$ , whereas that with 5 µM curcumin was  $0.70 \pm 0.58$ . For H-111-TC, that was  $3.24 \pm 0.44$ , whereas that with 5 µM curcumin was  $0.65 \pm 0.28$ . GO-Y022 exhibited 2.78-fold higher potential of the apoptosis

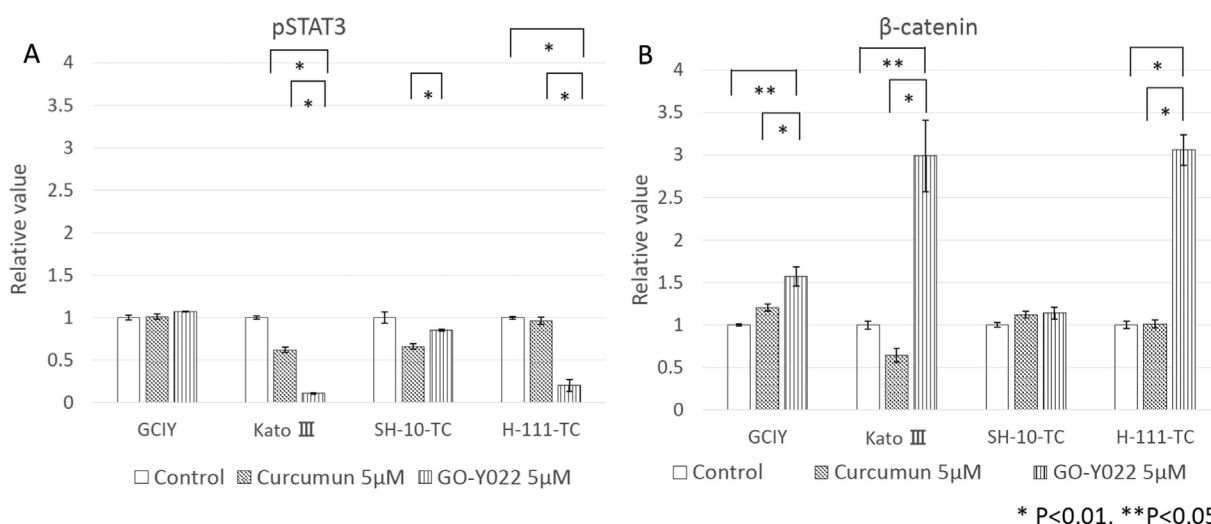


**Fig. 5.** Effects on the phosphorylation of STAT3 and β-catenin by GO-Y022. A. The levels of phosphorylated STAT3 (pSTAT3) were determined by ELISA methods. The amounts of pSTAT3 in the mock-treated cells (1% DMSO) treatment as a control are indicated as 1.0 (open rectangle). The relative values of pSTAT3 to the mock in each treated cells with 5 µM of curcumin (rectangle with diagonal line) and GO-Y022 (rectangle with vertical line) were indicated. The statistical significance is indicated by asterisks. B. The levels of β-catenin were determined by ELISA methods. The amounts of β-catenin in the mock-treated cells (1% DMSO) treatment as a control are indicated as 1.0 (open rectangle). The relative values of β-catenin to the mock in each treated cells with 5 µM of curcumin (rectangle with diagonal line) and GO-Y022 (rectangle with vertical line) were indicated. The statistical significance is indicated by asterisks.

induction than curcumin in GCIY. GO-Y022 also exhibited 15.6-fold and 4.98-fold higher apoptosis induction in KATO III and H-111-TC cell lines, respectively. However, for SH-10-TC, that was  $9.40 \pm 0.15$ , whereas that with  $5 \mu\text{M}$  curcumin was  $8.99 \pm 0.23$ . That was merely 1.05-fold higher than curcumin. So we confirmed the data by FACS analysis (Fig. S1). Apoptosis/necrosis fraction was 25.5% in  $5 \mu\text{M}$  of curcumin treated SH-10-TC cells, whereas that was 28.8% in the mock-treated cells. On the other hand, that was 34.9% in  $5 \mu\text{M}$  GO-Y022 treated SH-10-TC cells. Further, that was 45.3% in  $10 \mu\text{M}$  GO-Y022 treated SH-10-TC cells, whereas that was 37.9% in  $10 \mu\text{M}$  curcumin treated SH-10-TC cells. Similar result was obtained and indicated that SH-10-TC cells was sensitive to GO-Y022 to induce apoptosis as well as curcumin.

Supplementary data associated with this article can be found, in the online version, at <https://doi.org/10.1016/j.jff.2018.09.033>.

The apoptosis induction might be one of the causes of growth inhibition of GO-Y022.

### 3.3. In vitro effects on the STAT3 phosphorylation and $\beta$ -catenin activation with GO-Y022

Several lines of evidence suggest that the suppression of the  $\beta$ -catenin pathway and phosphorylation of STAT3 at Tyr705 contribute to the inhibition of gastric carcinogenesis (Clements, Wang, & Sarnaik, 2002; Tye, Kennedy, & Najdovska, 2012). As our newly synthesized curcumin analogs have similar diarylpentanoid structures, they are supposed to have same targets molecules. For examples, GO-Y030 and GO-Y031 have suppressive effects on the growth of gastrointestinal tumors. GO-Y031, another and more potent C5 curcumin analog that is not found in cooked curry, was previously reported to suppress the  $\beta$ -catenin activation and STAT3 phosphorylation (Uehara et al., 2014). GO-Y030 was shown to associate with the ATP binding site of STAT3 (Lin et al., 2011). Moreover, it was reported that *Helicobacter pylori*, a major cause of gastric cancer, activates STAT3 that plays an important role in gastric carcinogenesis (Zhao, Dong, & Kang, 2014). Thus, we

assessed the ability of GO-Y022 to inhibit the STAT3 phosphorylation and to degrade  $\beta$ -catenin in gastric cancer cell lines.

#### 3.3.1. Inhibition of pSTAT3

The relative pSTAT3 level per cell, compared with mock (1% DMSO) was  $0.111 \pm 0.011$  at  $5 \mu\text{M}$  of GO-Y022, in KATO III, whereas that was  $0.621 \pm 0.046$  in KATO III at  $5 \mu\text{M}$  of curcumin. The relative pSTAT3 level was  $0.850 \pm 0.016$  in SH-10-TC with  $5 \mu\text{M}$  GO-Y022, whereas that was  $0.661 \pm 0.046$  in SH-10-TC at  $5 \mu\text{M}$  curcumin. The relative pSTAT3 level was  $0.196 \pm 0.097$  in H-111-TC, whereas that was  $0.958 \pm 0.060$  in H-111-TC at  $5 \mu\text{M}$  curcumin. The relative pSTAT3 level was  $1.063 \pm 0.007$  in GCIY with  $5 \mu\text{M}$  GO-Y022, whereas that was  $1.002 \pm 0.040$  in GCIY at  $5 \mu\text{M}$  curcumin (Fig. 5A). Inhibition of pSTAT3 with  $5 \mu\text{M}$  of GO-Y022 was apparent in KATO III and H-111-TC, however that was not observed in SH-10-TC and GCIY.

The relationships among the  $\text{IC}_{50}$  values, the relative apoptosis induction (at  $5 \mu\text{M}$ ) and the relative inhibition of pSTAT3 (at  $5 \mu\text{M}$ ) varied among cell lines. To examine the effect of pSTAT3 inhibition on the gastric cancer cell lines, we used cryptotanshinone (CTS), a known STAT3 phosphorylation inhibitor (Donmez, Demirezen, & Beksac, 2016). The  $\text{IC}_{50}$  value of CTS for KATO III was  $4.29 \mu\text{M}$ . That for GCIY was  $14.02 \mu\text{M}$ . That for SH-10-TC was  $6.91 \mu\text{M}$ . However, that for H-111-TC was  $> 100.0 \mu\text{M}$  (Fig. S2).

#### 3.3.2. Effect on $\beta$ -catenin

GO-Y030 and GO-Y031 can induce the degradation of  $\beta$ -catenin. Therefore, we also examined the degradation of  $\beta$ -catenin with GO-Y022.

At  $5 \mu\text{M}$ , GO-Y022 did not decrease the relative levels of activated  $\beta$ -catenin per cell (Fig. 5B); the relative levels to the control (1% DMSO) was  $1.566 \pm 0.163$  in GCIY. That was  $2.988 \pm 0.593$  in KATO III. Those were  $1.136 \pm 0.099$  in SH-10-TC, and  $3.057 \pm 0.252$  in H-111-TC cells, respectively. In contrast, that with  $5 \mu\text{M}$  curcumin in GCIY was  $1.198 \pm 0.060$ , that in KATO III was  $0.638 \pm 0.112$ , that in SH-10-TC was  $1.117 \pm 0.056$ , and that in H-111-TC was  $1.009 \pm 0.065$

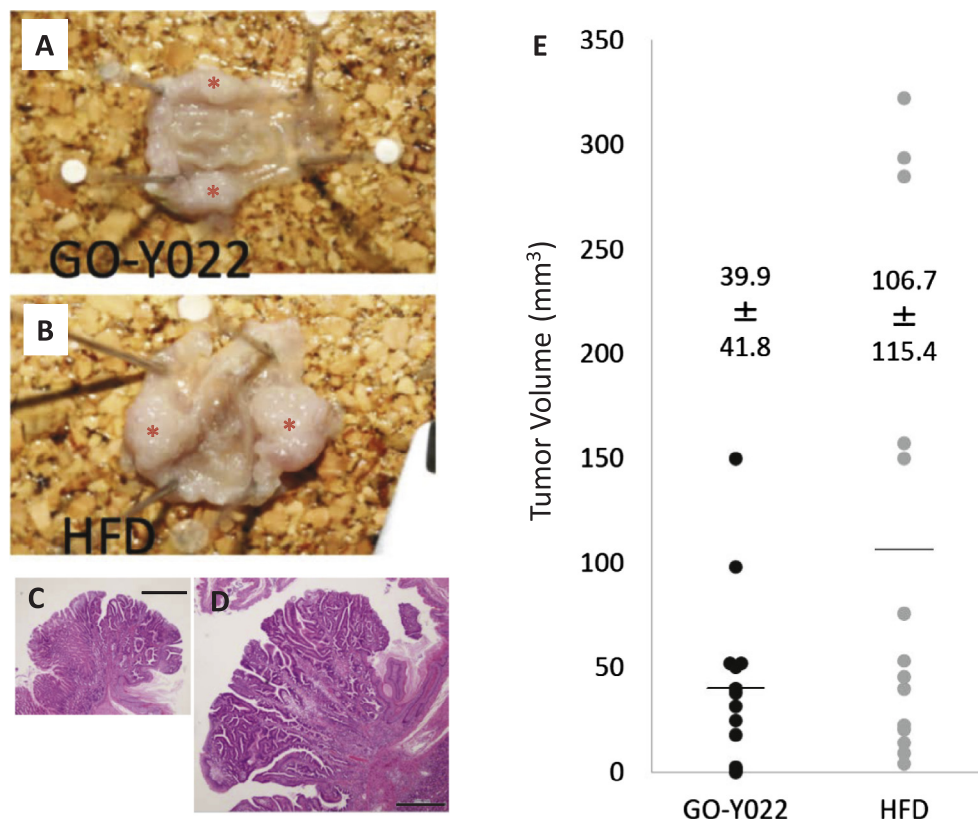


**Fig. 6.** The *in vivo* inhibition of gastric cancer in a mouse model with the oral administration of GO-Y022. A, Representing appearance of GO-Y022-treated gastric tumors. Twenty-five milligram of GO-Y022 was mixed in 5 g of HFD were given daily and freely to each mouse. Astarisks indicate the tumors. The average tumor incidence was two in a mouse. B, HFD alone-treated gastric tumor. Red asterisk indicates tumor. C and D, pathological views of A and B, respectively. Bars indicate 500  $\mu\text{m}$ . E, The volume of each tumor in the GO-Y022-treated ( $n = 7$ ) and the HFD-mice ( $n = 6$ ). The average volume with standard deviation of each group is indicated ( $p = 0.0585$ ). (For interpretation of the references to colour in this figure legend, the reader is referred to the web version of this article.)

(Fig. 5B). In the cases of the 5  $\mu$ M curcumin treatment, the levels of activated  $\beta$ -catenin per cell were not decreased and comparable with the control. Different from pSTAT3,  $\beta$ -catenin was activated in the surviving cells treated with 5  $\mu$ M GO-Y022. This phenomenon was similar to the observation where  $\beta$ -catenin showed intense positivity in the non-apoptotic epithelial cells around the apoptotic cells (Ge, Yang, & Chen, 2015).

Degradation of  $\beta$ -catenin by GO-Y022 was not observed. The action mechanisms of GO-Y022 was different from another curcumin analog such as GO-Y030 and GO-Y031 in this aspect.

### 3.4. *In vivo* inhibitory potential of GO-Y022 in a mouse model of gastric cancer

We assessed the *in vivo* ability of GO-Y022 to inhibit gastric carcinogenesis in Gan mice that were freely administered 0.5% (weight/weight) GO-Y022 orally for 8 weeks. Histopathologically, all gastric tumors were suggested to be adenocarcinomas. As the tumors grew in a block, it became difficult to count the multiplicity of tumors; thus, we evaluated the volume of tumors. The average volume of gastric tumors in mice treated with GO-Y022 for 8 weeks was  $39.9 \pm 41.8$  (range: 0.5–150.0)  $\text{mm}^3$ , whereas that in mock-treated mice was  $106.7 \pm 115.4$  (range: 4.0–322.5)  $\text{mm}^3$  ( $p = 0.059$ ; Fig. 6), which suggested that GO-Y022 could apparently inhibit the gastric cancer growth *in vivo*. In addition, we determined the expression of GO-Y022-target molecules  $\beta$ -catenin and pSTAT3 by immunohistochemistry (Fig. S3). The disappearance of the  $\beta$ -catenin signal in the cytosol, which revealed the accumulation of  $\beta$ -catenin, an indicator of the  $\beta$ -catenin activation, was not apparent. However, the inhibition of the nuclear staining for pSTAT3 was apparently detected by immunohistochemistry (IHC). By IHC of Gan mice treated with HFD, it was shown that pStat3 in the nucleus was observed in many cells, however that was not so frequently observed in the epithelial cells in mice treated with GO-Y022 (Fig. S3A and B). Quantitation of the positivity of pStat3 expression indicated that the percentage of pStat3-positive cells was  $64.4 \pm 10.1\%$  (range: 54.0–82.0) in Gan mice fed with mock, whereas that was  $20.3 \pm 15.2\%$  (range: 2.0–38.0) in Gan mice fed with GO-Y022 ( $p = 0.001$ , Fig. S3C). This data showed that GO-Y022 could inhibit phosphorylation of Stat3 *in vivo*, and that is a candidate target molecule of GO-Y022.

### 3.5. Localization of GO-Y022 in mice

We assessed localization of GO-Y022 in Gan mice by HPLC. The tissue GO-Y022 concentrations in the heart, kidney, liver, spleen, as well as the peripheral blood, were negligible in the treated mice (Fig. 7). Conversely, GO-Y022 was detected in the digestive tract, including the esophagus, stomach, and small and large intestines of the treated mice (Fig. 7). In addition, the concentrations of GO-Y022 ranged from 647 ng/g (tissue in the esophagus), 570–2590 ng/g (tissue in the stomach), to 40–446 ng/g (tissue in the small intestine; Fig. 7). Detection of GO-Y022 in the tissues varied among samples. We guess this variation was influenced by free eating, not gavage. Actually, the left over of feed was different among mice, and the timing of eating might be varied.

GO-Y022 really could not be absorbed? We added a next experiment to examine the existence of GO-Y022 including their possible metabolites. In this experiment, we administrated 5 mg of GO-Y022 with gavage mixed with methylcellulose. The blood samples were collected at 6 points of the time, those were just before of administration, 1 h, 2 h, 4 h, 8 h, and 24 h after administration. To identify the metabolites of GO-Y022, we set control groups administrated with vehicle methylcellulose alone for comparison. When additional peaks are observed by HPLC, those are considered as GO-Y022 relating metabolites. However, there were no peaks corresponding to GO-Y022 and additional peaks in the blood samples obtained from 6 time points (Fig. S4). We have

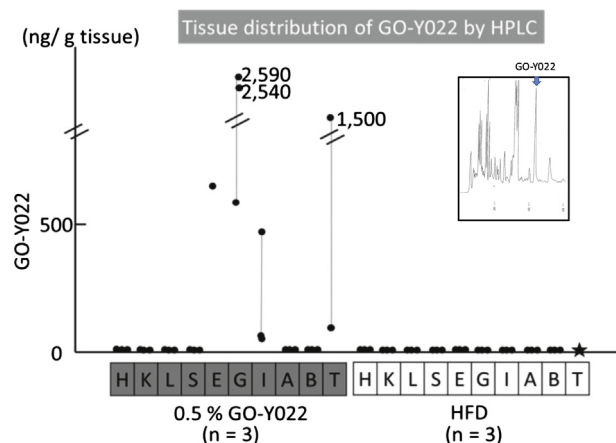


Fig. 7. Tissue distribution of GO-Y022. The data shows the tissue distribution of GO-Y022 in Gan mice (GO-Y022 treated mice ( $n = 3$ ) and mock-diet mice ( $n = 3$ )). H, heart; K, kidney; L, liver; S, spleen; E, esophagus; G, gastric lumen; I, intestine; A, ascending colon; B, blood; T, tumor. Each dot and a star indicate an individual mouse. The result of HPLC analysis is indicated in the inset, representatively.

judged GO-Y022 and its metabolites were not detected in the blood.

Orally administrated GO-Y022 acted topically in the luminal epithelia of the digestive organs. Finally, the tumor concentrations of GO-Y022 ranged 80–1500 ng/g tissue.

### 3.6. Safety profile of GO-Y022

First, we examined the effect of GO-Y022 on the normal gastric epithelium using a primary culture of HGaEpC. GO-Y022 has a growth inhibitory effect on HGaEpC, and the  $\text{IC}_{50}$  values was 3.08  $\mu$ M (Fig. S5). Spheroids of HGaEpC were observed at 10  $\mu$ M, but they were absent at 50  $\mu$ M. The cells were entirely killed at 50  $\mu$ M.

We assessed the hepatic and renal toxicity profiles of GO-Y022 by measuring Cre, AST, ALT, LDH, and T-Bil levels (Fig. 8).

While Cre levels were 0.12–0.20 mg/dL in GO-Y022-treated mice, they were 0.14–0.20 mg/dL in mock-treated mice. The AST levels were 52–108 IU/L in GO-Y022-treated mice and they were 60–186 IU/L in mock-treated mice. In addition, the ALT levels were 18–70 IU/L in GO-Y022-treated mice and 18–126 IU/L in mock-treated mice. Those of LDH were 322–758 IU/L in GO-Y022-treated mice and they were 334–674 IU/L in mock-treated mice. Finally, the T-Bil levels were 0.04–0.14 mg/dL in GO-Y022-treated mice and 0.06–0.10 mg/dL in mock-treated mice.

The levels of serum AST and ALT are parameters of liver damage. In both mice, the levels of AST and ALT were higher than the normal limits. That was because HFD diet induced a fatty change of liver in both mice. However, there were no differences between the mock-treated mice and in GO-Y022-treated mice. We concluded that additional liver damage was not induced in GO-Y022-treated mice.

The serum Cre level is a parameter of renal damage. The serum creatinine levels were within the normal limit, and there were no differences between both groups. We considered that no renal damage was induced in GO-Y022-treated mice.

These data suggested that additional damages to the liver or kidney were not induced in GO-Y022-treated mice. Furthermore, body weights of GO-Y022-treated mice ranged 23.7–37.6 (average:  $32.3 \pm 5.88$ ) g, whereas those of the mock mice ranged 21.7–46.1 (average:  $33.9 \pm 13.8$ ) g; we observed no significant difference in the body weight between the two groups. Overall, these findings demonstrated that 0.5% GO-Y022 administrated had a safe profile in mice.

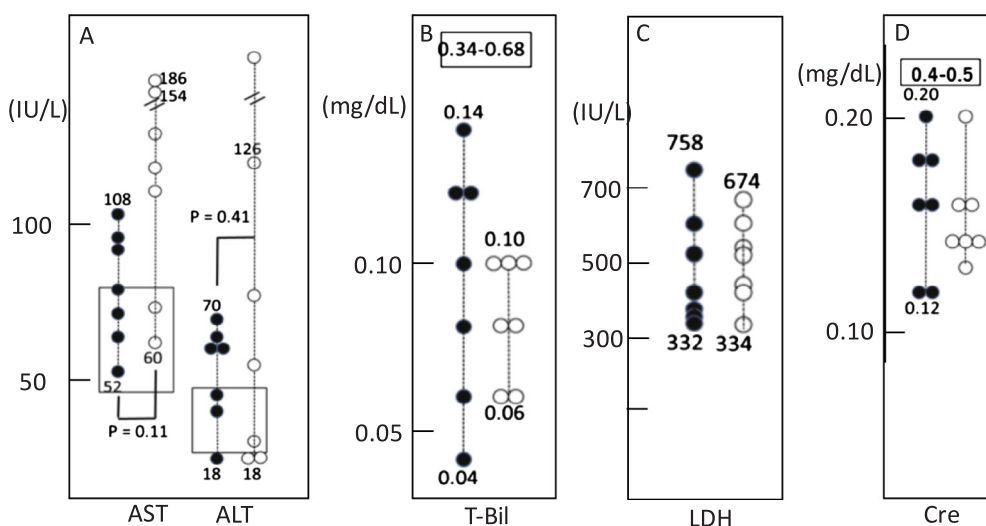


**Fig. 8.** Laboratory parameters in GO-Y022-fed mice and HFD-fed mice. A, Data of AST and ALT levels. B, Data of total bilirubin (T-Bil) level. C, Data of LDH. D, Data of creatinine (Cre). Black dot indicates GO-Y022-fed mouse and white dot indicates HFD-fed mouse. The numbers surrounded by rectangle indicate the normal limit of each parameter. The data were obtained from seven mice in each group.

### 3.7. GO-Y022, as an ingredient of cooked curry

We determined the GO-Y022 content in cooked curry, which is a regularly consumed food prepared from commercially available retort-pouch preparations, by mass spectrometry. Specifically, we tested nine different curries, revealing that the GO-Y022 concentrations varied from zero to 98  $\mu\text{g}/100\text{ g}$  curry (Table S2). In addition, heating the curry at 250  $^{\circ}\text{C}$  for 20 min led to an increase in the GO-Y022 content to 110  $\mu\text{g}/100\text{ g}$  curry. Although the amount of GO-Y022 in the commercially available curries was minimal, we already experienced eating GO-Y022, a C5 analog of curcumin.

## 4. Discussion

This study demonstrates that dietary GO-Y022, a C5 curcumin analog, inhibited the gastric cancer growth both *in vitro* and *in vivo*. The growth suppression potential of GO-Y022 was higher than that of curcumin in four gastric cancer cell lines. Except for GCIY, 5  $\mu\text{M}$  GO-Y022 decreased the growth < 50% of the control. In addition, it was a more potent inducer of apoptosis compared with curcumin in all cell lines. Histopathologically, GCIY is a poorly differentiated adenocarcinoma and belongs to a diffuse type based on the Lauren classification (Maki, Nobutake, & Ken-ichi, 2013). Kato III is a signet-ring cell carcinoma and belongs to a diffuse type. SH-10-TC is a mucinous adenocarcinoma and belongs to a diffuse type. H-111-TC is a well-differentiated adenocarcinoma and belongs to an intestinal type. We anticipated that GO-Y022 could be more effective in some gastric cancer cell lines, depending on the pathological subtypes. In this study, we elucidated that GO-Y022 suppressed pSTAT3 *in vitro* except GCIY, and *in vivo*.

Inhibition of pSTAT3 with 5  $\mu\text{M}$  of GO-Y022 was strongest in KATO III among four cell lines, and KATO III was also most sensitive to CTS. Apoptosis induction with 5  $\mu\text{M}$  of GO-Y022 in KATO III was also highest. KATO III is most sensitive to pSTAT3 inhibition including GO-Y022 (Table S1). Inhibition of pSTAT3 with 5  $\mu\text{M}$  of GO-Y022 was not observed in GCIY, and GCIY was also rather resistant to CTS. GCIY seemed to be most resistant to pSTAT3 inhibition, including GO-Y022. Apoptosis induction with 5  $\mu\text{M}$  of GO-Y022 in GCIY was lower.

Inhibition of pSTAT3 with 5  $\mu\text{M}$  of GO-Y022 was lesser in SH-10-TC, however SH-10-TC was relatively sensitive to CTS. Apoptosis induction with 5  $\mu\text{M}$  of GO-Y022 in SH-10-TC was stronger. SH-10-TC is also sensitive to pSTAT3 inhibition (Table S1). Finally, inhibition of pSTAT3 with 5  $\mu\text{M}$  of GO-Y022 was stronger in H-111-TC, however H-111-TC was most resistant to CTS growth inhibition. H-111-TC seemed to be most resistant to pSTAT3 inhibition. Although GO-Y022 suppressed pSTAT3 expression, apoptosis induction with 5  $\mu\text{M}$  of GO-Y022 in H-

111-TC was lowest. There might be some resistant mechanisms to apoptosis occurred in the downstream signaling of pSTAT3. It is speculated that growth suppression was due to different mechanism from apoptosis in H-111-TC (Table S1).

Inhibition of pSTAT3 with GO-Y022 might depend on cell lines. The resistance to a STAT3 inhibitor, CTS varied among cell lines. These differences might be reflected by the molecular backgrounds of the cells. The underlying mechanisms of sensitivity should be elucidated.

In Gan mice, together with the prostaglandin E synthase (PTGES) overexpression, Wnt signaling and cyclooxygenase-2 (Cox2) expression contributed to gastric carcinogenesis. Reportedly, a positive feedback loop between STAT3 and COX2 contributes to gastric tumorigenesis (Xiong, Du, & Sun, 2014). Furthermore, the Wnt/ $\beta$ -catenin pathway was reported to cross-talk with STAT3 signaling in the retina (Fragoso, Patel, & Nakamura, 2012). Moreover, PTGES-derived prostaglandin E2 was illustrated to stimulate STAT3 to promote apoptosis of podocytes (Yu, Wu, & Wang, 2017). Notably, STAT3 plays a vital role in the intersection of the Wnt, Cox2, and PTGES signaling pathways and could affect them. This study suggests pSTAT3 as one of the key molecules controlling gastric carcinogenesis and that the inhibition of pSTAT3 could suppress the growth of gastric cancer. In GCIY, the inhibition of pSTAT3 with GO-Y022 was insufficient, and GCIY might be relatively resistant to GO-Y022.

This study confirmed that the dietary GO-Y022 is present in commercially available curry pastes. Evidently, GO-Y022 can be ingested by humans. We observed no adverse effects with the administration of 5 mg GO-Y022 to a 20 g mouse per day. A phase I clinical trial reported the tolerability of a daily curcumin dose of 8 g (Cheng, Hsu, & Lin, 2001). However, whether an equivalent GO-Y022 dose is safe in humans remains unclear.

GO-Y022 is insoluble in water and, thus, cannot be administrated intravenously. This study demonstrates that the blood GO-Y022 concentration was insignificant. Nonetheless, orally administrated GO-Y022 can be directly transferred into the tumors, as well as to the luminal surface of the digestive tract. However, we did not detect apparent toxicity in the epithelial cells of the digestive tract. Moreover, GO-Y022 had somewhat a growth suppressive effect on the primary gastric epithelial cells less than 10  $\mu\text{M}$ , but a killing effect was apparent at as high as 50  $\mu\text{M}$ . These aspects of GO-Y022 highlight its benefit in controlling malignancies of the digestive tract by topical application. Furthermore, contingent upon the absence of long-term toxic effects, dietary GO-Y022 should be considered for chemoprevention of gastrointestinal cancers.

In this study, we also assessed whether GO-Y022 could be ingested as a supplement by determining the amount of GO-Y022 in

commercially available curry pastes and determined that its concentration ranged from zero to 100 µg in 100 g curry paste, which varied among the samples. Notably, there remains a room for the development of better recipes for curry paste with higher GO-Y022 concentrations.

Whether C5 analogs other than dietary GO-Y022 can be ingested safely remains unexplored. Recently, we developed the most potent C5 analog (1E, 4E)-1,5-bis-(3,5-(bismethoxymethoxyphenyl) penta-1,4-dien-3-one (GO-Y030) with 10 and 2 times the potency of curcumin and GO-Y022, respectively, to inhibit the growth of various cancer cells (Ohori et al., 2006). The oral administration of GO-Y030 at the same dose as GO-Y022 did not correlate with any apparent toxicities in mouse models. Of note, GO-Y030 is insoluble in water and is not absorbed systemically. If the safety profile of the orally administered GO-Y030 is found to be similar to that of GO-Y022, GO-Y030 could be a better alternative in the prevention of malignancies of the digestive tract by the topical use through oral administration.

## 5. Conclusions

A diarylpentanoid analog of curcumin, GO-Y022 is included in curry, and human beings have been eating it for many thousands years. This compound formed from pyrolysis of curcumin. It has a growth inhibitory and an apoptosis inducing effects on gastric cancer cells mainly via pSTAT3 inhibition. GO-Y022 could inhibit the growth of gastric tumors in mouse model with safe.

## Acknowledgments

We thank Mrs. Ikuko Ogasawara for her technical assistance. This study was partially supported by Akita Industrial/Academic/Governmental Research Project on Developing Innovations, Joint Research and Promotion Project on Creating New Technologies and Industries, and Yamasaki Spice Promotion Foundation. This work was also supported by JSPS KAKENHI Grant Number JP 16H06276. The authors also thank Enago (<http://www.enago.jp>) for review and revision of the language.

## Ethical issues

All animal experiments were performed humanely and complied with the guidelines set by Akita University and were approved by the associated ethics committee.

## Disclosure of potential conflicts of interest

There are no conflicts of interest in this study.

## References

- Cheng, A. L., Hsu, C. H., Lin, J. K., et al. (2001). Phase I clinical trial of curcumin, a chemopreventive agent, in patients with high-risk or pre-malignant lesions. *Anticancer Research*, *21*, 2895–2900.
- Clements, W. M., Wang, J., Sarnaik, A., et al. (2002). b-Catenin mutation is a frequent

- cause of Wnt pathway activation in gastric cancer. *Cancer Research*, *62*, 3503–3506.
- Cunningham, D., Starling, N., Rao, S., et al. (2008). Capecitabine and oxaliplatin for advanced esophagogastric cancer. *The New England Journal of Medicine*, *358*, 36–46.
- Dahmke, I. N., Boettcher, S. P., Groh, M., et al. (2014). Cooking enhances curcumin anticancerogenic activity through pyrolytic formation of “deketeene curcumin”. *Food Chemistry*, *151*, 514–519.
- Donmez, H. G., Demirezen, S., & Beksac, M. S. (2016). The relationship between beta-catenin and apoptosis: A cytological and immunocytochemical examination. *Tissue and Cell*, *48*, 160–167.
- Euhus, D. M., Hudd, C., LaRegina, M. C., et al. (1986). Tumor measurement in the nude mouse. *Journal of Surgical Oncology*, *31*, 229–234.
- Ferlay, J., Soerjomataram, I., Dikshit, R., et al. (2015). Cancer incidence and mortality worldwide: Sources, methods and major patterns in GLOBOCAN 2012. *International Journal of Cancer*, *136*, E359–E386.
- Fragoso, M. A., Patel, A. K., Nakamura, R. E., et al. (2012). The Wnt/β-catenin pathway cross-talks with STAT3 signaling to regulate survival of retinal pigment epithelium cells. *PLoS One*, *7*, e46892.
- Ge, Y., Yang, B., Chen, Z., et al. (2015). Cryptotanshinone suppresses the proliferation and induces the apoptosis of pancreatic cancer cells via the STAT3 signaling pathway. *Molecular Medicine Reports*, *12*, 7782–7788.
- Hundahl, S. A., Phillips, J. L., & Menck, H. R. (2000). The National Cancer Data Base Report on poor survival of U.S. gastric carcinoma patients treated with gastrectomy: Fifth Edition American Joint Committee on Cancer staging, proximal disease, and the “different disease” hypothesis. *Cancer*, *88*, 921–932.
- Japanese Gastric Cancer Association (2017). Japanese gastric cancer treatment guidelines 2014 (ver. 4). *Gastric Cancer*, *20*, 1–19.
- Kudo, C., Yamakoshi, H., Sato, A., et al. (2011). Synthesis of 86 species of 1,5-diaryl-3-oxo-1,4-pentadienes analogs of curcumin can yield a good lead in vivo. *BMC Pharmacology*, *11*, 4.
- Kunnumakkara, A. B., Bordoloi, D., Harsha, C., et al. (2017). Curcumin mediates anticancer effects by modulating multiple cell signaling pathways. *Clinical Science*, *131*, 1781–1799.
- Lin, L., Liu, Y., Li, H., et al. (2011). Targeting colon cancer stem cells using a new curcumin analogue, GO-Y030. *British Journal of Cancer*, *105*, 212–220.
- Maki, K. S., Nobutake, Y., Ken-ichi, I., et al. (2013). Cathepsin E is a marker of gastric differentiation and signet-ring cell carcinoma of stomach: A novel suggestion on gastric tumorigenesis. *PLoS One*, *8*, e56766.
- Mohamed, S. I. A., Jantan, I., & Haque, M. A. (2017). Naturally occurring immunomodulators with antitumor activity: An insight on their mechanisms of action. *International Immunopharmacology*, *50*, 291–304.
- Ohori, H., Yamakoshi, H., Tomizawa, M., et al. (2006). Synthesis and biological analysis of new curcumin analogues bearing an enhanced potential for the medicinal treatment of cancer. *Molecular Cancer Therapeutics*, *5*, 2563–2571.
- Oshima, H., Matsunaga, A., Fujimura, T., et al. (2006). Carcinogenesis in mouse stomach by simultaneous activation of the Wnt signaling and prostaglandin E2 pathway. *Gastroenterology*, *131*, 1086–1095.
- Shibata, H., Yamakoshi, H., Sato, A., et al. (2009). Newly synthesized curcumin analog has improved potential to prevent colorectal carcinogenesis in vivo. *Cancer Science*, *100*, 956–960.
- Tye, H., Kennedy, C. L., Najdovska, M., et al. (2012). STAT3-driven upregulation of TLR2 promotes gastric tumorigenesis independent of tumor inflammation. *Cancer Cell*, *22*, 466–478.
- Uehara, Y., Inoue, M., Fukuda, K., et al. (2014). Inhibition of β-catenin and STAT3 with a curcumin analog suppresses gastric carcinogenesis in vivo. *Gastric Cancer*, *18*, 774–783.
- Van Cutsem, E., Moiseyenko, V. M., Tjulandin, S., et al. (2006). Phase III study of docetaxel and cisplatin plus fluorouracil compared with cisplatin and fluorouracil as first-line therapy for advanced gastric cancer: A report of the V325 study group. *Journal of Clinical Oncology*, *24*, 4991–4997.
- Xiong, H., Du, W., Sun, T. T., et al. (2014). A positive feedback loop between STAT3 and cyclooxygenase-2 gene may contribute to Helicobacter pylori-associated human gastric tumorigenesis. *International Journal of Cancer*, *134*, 2030–2040.
- Yu, J., Wu, Y., Wang, L., et al. (2017). mPGES-1-derived prostaglandin E2 stimulates Stat3 to promote podocyte apoptosis. *Apoptosis*, *22*, 1431–1440.
- Zhang, J. Y., Lin, M. T., Zhou, M. J., et al. (2015). Combinational treatment of curcumin and quercetin against gastric cancer MGC-803 cells in vitro. *Molecules*, *20*, 11524–11534.
- Zhao, J., Dong, Y., Kang, W., et al. (2014). Helicobacter pylori-induced STAT3 activation and signalling network in gastric cancer. *Oncoscience*, *1*, 468–475.